Inorg. Chem. **2002**, *41*, 3673–3683

A Solvent-Controlled Switch of Manganese Complex Assemblies with a β-Diketonate-Based Ligand

Guillem Aromí,[†] Patrick Gamez,[†] Olivier Roubeau,[†] Paula Carrero Berzal,[†] Huub Kooijman,[‡] Anthony L. Spek,[‡] Willem L. Driessen,[†] and Jan Reedijk*[,†]

Leiden Institute of Chemistry, Gorlaeus Laboratories, Leiden University, PO Box 9502, 2300 RA Leiden, The Netherlands, and Bijvoet Center for Biomolecular Research, Crystal and Structural Chemistry, Utrecht University, Padualaan 8, 3584 CH Utrecht, The Netherlands

Received January 17, 2002

The coordination properties of the new polynucleating ligand H_3**L1** (1,3-bis(3-oxo-3-phenylpropionyl)-2-hydroxy-5-methylbenzene) with $Mn^{II/III}$ are described. Depending on the solvent used, the reaction of H_3**L1** with $Mn(OAc)_2$ yields either of the two new multinuclear assemblies $[Mn_2(H\mathbf{L1})_2(py)_4]$ (**1**) and $[Mn_3(H\mathbf{L1})_3]$ (**2**), as revealed by X-ray crystallography. The structure of **2** is remarkable in that it shows a unique asymmetric triple-stranded helicate. Complexes **1** and **2** can be interconverted by controlling the solvent of the reaction system, and therefore, this ensemble constitutes an interesting externally addressable switch. In the presence of Mn^{III}/pyridine, partial degradation of H_3**L1** occurs via oxidative cleavage, and the new complex $[Mn_2(\mathbf{L2})_2(py)_4]$ (**3**) is formed. The crystal structure of this complex has shown the fully deprotonated form of the new donor H_3**L2** (3-(3-oxo-3-phenylpropionyl)-5-methylsalicylic acid). From the same reaction, the Mn^{II} complex **1** is also obtained. A rational synthesis of H_3**L2** is reported, and this has been used to prepare **3** in high yields, directly from its components. Variable-temperature magnetic susceptibility (χ_m) measurements were performed on complexes **1**–**3** under a magnetic field of 1 kG. The data for each complex were fit to the appropriate χ_m vs T theoretical equation, respectively. In **1**, the Mn^{II} ions are uncoupled, with $g = 2.01$. The data from **2** were fit by assuming the presence of an exchange coupled $Mn^{II}\cdots Mn^{II}$ pair next to a magnetically isolated Mn^{II} center. The fit gave $J = -2.75$ cm^{-1}, $g_{12} = 1.97$, and $g_3 = 1.92$, respectively. In **3**, two models fit the experimental data. In the most satisfactory, the Mn^{III} ions are coupled antiferromagnetically with $J = -1.48$ cm^{-1} and $g = 1.98$ and a term for weak ferromagnetic intermolecular exchange is included with $zJ' = 0.39$ cm^{-1}. The other model contemplates the presence of two uncloupled zero field split Mn^{III} ions.

Introduction

One of the most prolific branches of supramolecular chemistry is that where the main chemical interaction cementing the construction of complicated molecular architectures from simpler components is the coordination bond.[1,2] In this context, the engineering of polynucleating ligands containing a suitable set of donors, appropriately distributed for the attainment of the desired final structure, is instrumental. Along these lines, the area of molecular magnetism is benefiting from this powerful synthetic methodology as well, by the nonserendipitous creation of transition-metal aggregates with predetermined structures and interesting magnetic properties.[3−7] A major goal remains that of producing molecular systems that change their magnetic properties reversibly as a response to external stimuli. A good example of this is the extensive family of Fe^{II} complexes, which, by virtue of a spin-crossover process, change their magnetic susceptibility upon light irradiation or temperature

* To whom correspondence should be addressed. E-mail: reedijk@chem.leidenuniv.nl; snellenb@chem.leidenuniv.nl (secretary).
† Leiden University.
‡ Utrecht University.

(1) Sauvage, J.-P.; Hosseini, M. W. In *Comprehensive Supramolecular Chemistry*; Lehn, J.-M., Ed.; Pergamon Press: Oxford, U.K., 1995; Vol. 9.
(2) Holliday, B. J.; Mirkin, C. A. *Angew. Chem., Int. Ed.* **2001**, *40*, 2022.
(3) Zhao, L.; Xu, Z. Q.; Thompson, L. K.; Miller, D. O. *Polyhedron* **2001**, *20*, 1359.
(4) Xu, Z. Q.; Thompson, L. K.; Miller, D. O. *Chem. Commun.* **2001**, 1170.
(5) Peng, S. M.; Wang, C. C.; Jang, Y. L.; Chen, Y. H.; Li, F. Y.; Mou, C. Y.; Leung, M. K. *J. Magn. Magn. Mater.* **2000**, *209*, 80.
(6) Waldmann, O.; Hassmann, J.; Muller, P.; Volkmer, D.; Schubert, U. S.; Lehn, J.-M. *Phys. Rev. B: Condens. Matter* **1998**, *58*, 3277.
(7) Saalfrank, R. W.; Trummer, S.; Reimann, U.; Chowdhry, M. M.; Hampel, F.; Waldmann, O. *Angew. Chem., Int. Ed.* **2000**, *39*, 3492.

10.1021/ic0200491 CCC: $22.00
Published on Web 06/14/2002

change.[8,9] Most of the ligands used in the area of coordination supramolecular chemistry are based on nitrogen donors. Compared to these, considerably less polytopic ligands have been prepared combining nitrogen with oxygen donors or based entirely on the latter. The series of ligands incorporating several catechol groups in their structure, used extensively in the construction of metallohelicates,[10] are, perhaps, among the most representative of them. We have recently initiated a program aimed at the design and synthesis of novel multinucleating ligands for the rational preparation of new transition-metal aggregates with interest in the area of magnetism. For this, it was intended to capitalize on the excellent chelating properties of the β-diketone unit by strategically combining several of them on the same molecule, along with other donating groups. Thus, a successful high-yield route to a new compound has been finalized, incorporating two 1,3-dicarbonyl moieties and a phenol group in its molecular structure, leading to the symmetric O-pentadentate ligand H_3**L1** (see structures following).[11] A few related bis(β-diketone) molecules have been reported to template the formation of supramolecular assemblies such as inclusion cages,[12−14] triple-stranded helicates,[14,15] or even octanuclear complexes.[16] The ligand H_3**L1** was prepared with the intention of using its basic forms to direct the assembly of linear arrays of closely spaced transition metals. Such type of molecular topology has been achieved with great success in the past, by use of oligo-α-pyridylamine ligands in combination with a variety of metals.[5,17,18]

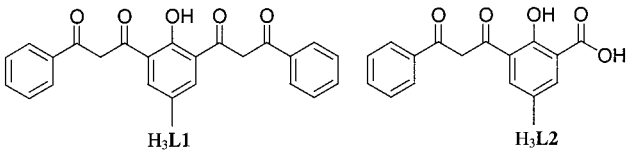

In this paper, the initial efforts to explore the coordination properties of the new ligand H_3**L1** with manganese in the oxidation states 2+ and 3+ are reported. The crystal structure and magnetic properties of the new polynuclear assemblies $[Mn_2(H\mathbf{L1})_2(py)_4]$ (**1**) and $[Mn_3(H\mathbf{L1})_3]$ (**2**) are presented. These two species undergo reversible interconversion triggered by the nature of the solvent in use. The trinuclear compound shows an asymmetric array of Mn^{II} atoms wrapped around by three $(H\mathbf{L1})^{2-}$ ligands in the form of a triple-stranded helix that represents a new topology within the family of coordination helicates. The new dinuclear Mn^{III} complex $[Mn_2(\mathbf{L2})_2(py)_4]$ (**3**) is also introduced, which contains the fully deprotonated form of a second new ligand (H_3**L2**; see previous structure). This ligand results from the degradation of H_3**L1** under the reaction conditions, and a rational synthetic route for its direct preparation is also reported. Portions of this work have been previously communicated.[19,20]

Experimental Section

Syntheses. All manipulations were performed under aerobic conditions using materials as received unless indicated otherwise. $NBu^n_4MnO_4$ was prepared according to a procedure reported in the literature.[21] The preparation of 1,3-bis(3-oxo-3-phenylpropionyl)-2-hydroxy-5-methylbenzene (H_3**L1**) is described in a separate article.[11]

5-Methylacetylsalicylic Acid. To a slurry of 5-methylsalicylic acid (5.9 g, 39 mmol) in acetic anhydride (12 mL) was added a catalytic amount of concentrated sulfuric acid (~50 μL). The mixture slowly turned into a dark solution to finally become a thick paste, to which was added water under vigorous stirring. A white solid was collected by filtration and dried in air. A second crop of the product was obtained from the filtrate as a very fine white powder that precipitated later. The yield was 98%.

IR (neat): ν (cm^{-1}) = 1756 vs, 1684 vs, 1373 s, 1295 s, 1280 s, 1225 vs, 1199 vs, 1136 s, 1085 s, 1015 s, 898 s, 844 s, 761 w, 646 w, 598 w, 532 s. ^{1}H NMR ($CDCl_3$): δ (ppm) = 2.34 (s, 3H, CH_3), 2.40 (s, 3H, CH_3), 7.03 (d, 1H, $C_{arom}H$), 7.42 (dd, 1H, $C_{arom}H$), 7.91 (d, 1H, $C_{arom}H$).

^{13}C NMR ($CDCl_3$): δ (ppm) = 20.7 (CH_3), 21.0 (CH_3), 121.6 (C_{arom}), 123.7 (C_{arom}), 132.8 (C_{arom}), 135.5 (C_{arom}), 136.1 (C_{arom}), 149.0 (C_{arom}), 170.00 (C═O), 170.23 (C═O).

Anal. Calcd for $C_{10}H_{10}O_4$ (M_r = 194.18): C, 61.85; H, 5.19. Found: C, 61.70; H, 5.02.

ESI (*m*/*z*): 193, $[M - H]^-$; 253, $[M + AcO]^-$.

5-Methyl-3-acetylsalicylic Acid. In a two-necked 100 mL flask fitted with an Ar inlet and an exhaust outlet, 5-methylacetylsalicylic acid (2.5 g, 13 mmol) and $AlCl_3$ (5.2 g, 39 mmol) were mixed. Both solids were heated to 180 °C under mechanical stirring (*caution*: *brisk evolution of HCl gas took place at this stage!*) to form a very viscous dark-brown paste. The mixture was maintained at this temperature for approximately 3 h and was occasionally stirred with a glass stick. The system was then allowed to cool to room temperature, and the remaining solid was ground into a yellow powder, which was poured onto crushed ice (100 g) and concentrated HCl (25 mL). After the ice had melted, ethyl acetate (50 mL) was added and the mixture was stirred until a very fine suspension formed, followed by extraction with CH_2Cl_2. The organic phase was dried over $MgSO_4$ and evaporated to dryness. The product was obtained as a cream-colored solid in 85% yield.

IR (neat): ν (cm^{-1}) = 2970.2 w, 2902.0 w, 1688.8 w, 1668.3 vs, 1645.6 vs, 1588.3 vs, 1455.7 s, 1373.8 s, 1306.8 w, 1243.3 vs,

(8) Gütlich, P.; Garcia, Y.; Woike, T. *Coord. Chem. Rev.* **2001**, *219*, 839.
(9) Roubeau, O.; Stassen, A. F.; Gramage, I. F.; Codjovi, E.; Linares, J.; Varret, F.; Haasnoot, J. G.; Reedijk, J. *Polyhedron* **2001**, *20*, 1709.
(10) Albrecht, M. *Chem. Soc. Rev.* **1998**, *27*, 281.
(11) Aromí, G.; Gamez, P.; Carrero Berzal, P.; Driessen, W. L.; Reedijk, J. *Synlett.*, in press.
(12) Bailey, N. A.; Fenton, D. E.; Lay, J.; Roberts, P. B.; Latour, J.-M.; Limosin, D. *J. Chem. Soc., Dalton Trans.* **1986**, 2681.
(13) Maverick, A. W.; Buckingham, S. C.; Yao, Q.; Bradbury, J. R.; Stanley, G. G. *J. Am. Chem. Soc.* **1986**, *108*, 7430.
(14) Saalfrank, R. W.; Seitz, V.; Caulder, D. L.; Raymond, K. N.; Teichert, M.; Stalke, D. *Eur. J. Inorg. Chem.* **1998**, 1313.
(15) Grillo, V. A.; Seddon, E. J.; Grant, C. M.; Aromí, G.; Bollinger, J. C.; Folting, K.; Christou, G. *Chem. Commun.* **1997**, 1561.
(16) Saalfrank, R. W.; Low, N.; Trummer, S.; Sheldrick, G. M.; Teichert, M.; Stalke, D. *Eur. J. Inorg. Chem.* **1998**, 559.
(17) Cotton, F. A.; Daniels, L. M.; Murillo, C. A.; Wang, X. P. *Chem. Commun.* **1998**, 39.
(18) van Albada, G. A.; van Koningsbruggen, P. J.; Mutikainen, I.; Turpeinen, U.; Reedijk, J. *Eur. J. Inorg. Chem.* **1999**, 2269.
(19) Aromí, G.; Carrero Berzal, P.; Gamez, P.; Roubeau, O.; Driessen, W. L.; Kooijman, H.; Spek, A. L.; Reedijk, J. *Angew. Chem., Int. Ed.* **2001**, *40*, 3444.
(20) Aromí, G.; Gamez, P.; Roubeau, O.; Carrero Berzal, P.; Driessen, W. L.; Kooijman, H.; Spek, A. L.; Reedijk, J. *Eur. J. Inorg. Chem.* **2002**, 1046.
(21) Vincent, J. B.; Folting, K.; Huffman, J. C.; Christou, G. *J. Am. Chem. Soc.* **1986**, *25*, 996.

1188.9 vs, 974.7 s, 825.8 w, 798.1 vs, 717.8 s, 663.1 s, 587.1 s, 542.1 s, 480.3 w, 459.4 s, 431.7 s, 373.8 w.

^{1}H NMR ($CDCl_3$): δ (ppm) = 2.37 (s, 3H, CH_3), 2.71 (s, 3H, CH_3), 7.80 (d, 1H, $C_{arom}H$), 8.16 (d, 1H, $C_{arom}H$), ∼9.7 (s, very broad, 1H, COOH), 14.03 (s, 1H, C_{arom}−OH).

^{13}C NMR ($CDCl_3$): δ (ppm) = 20.2 (CH_3), 27.8 (CH_3), 116.1 (C_{arom}), 121.1 (C_{arom}), 129.1 (C_{arom}), 136.8 (C_{arom}), 139.7 (C_{arom}), 159.4 (C_{arom}OH), 167.2 (C═O), 204.2 (COOH).

Anal. Calcd for $C_{10}H_{10}O_4$ (M_r = 194.18): C, 61.85; H, 5.19. Found: C, 61.84; H, 5.17.

ESI (*m*/*z*): 195, $[M + H]^+$.

3-(3-Oxo-3-phenylpropionyl)-5-methylsalicylic Acid (H3L2). A 60% oil dispersion of NaH (2 g, 50 mmol) was stirred with hexanes (20 mL) in a two-necked 100 mL round-bottom flask fitted with a condenser. The solvent was removed under Ar with a special cannula filter. A solution containing 5-methyl-3-acetylsalicylic acid (1.99 g, 10 mmol) and ethyl benzoate (1.9 g, 12.6 mmol) in DME (dimethoxyethane, 50 mL) was then carefully added under Ar, and brisk evolution of H_2 could be observed. After completion of the addition, the yellow mixture was brought to reflux and gradually turned dark-orange. The reflux was maintained for ca. 20 h, after which the system was allowed to cool to room temperature. An orange, very fine precipitate was collected by filtration and suspended in a biphasic water/ether medium. The basic salts were neutralized with concentrated HCl under vigorous stirring until the aqueous phase became acidic. The two layers were separated, and the orange organic phase was dried over $MgSO_4$ and rotoevaporated. The remaining orange solid was stirred in EtOH (60 mL), and a fine yellow powder (0.46 g) was collected by filtration. A second crop of the compound (0.37 g) was obtained from the filtrate after it was left to stand at −20 °C for 3 days. The overall yield was 28%.

IR (neat): ν (cm^{-1}) = 1683.7 w, 1615.9 w, 1575.4 s, 1538.2 s, 1417.7 w, 1315.4 w, 1227.2 s, 1185.6 vs, 1158.0 vs, 1113.5 s, 871.8 w, 819.5 s, 799.9 s, 774.3 s, 730.6 w, 709.9 w, 680.6 vs, 613.6 vs, 552.0 w, 497.7 w, 373.3 w, 346.0 w.

^{1}H NMR (DMSO-d_6): δ (ppm) = 2.29 (s, 3H, CH_3), 7.43 (s, 1H, $C_{enol}H$), 7.54 (t, 2H, $C_{arom}H$), 7.63 (t, 1H, $C_{arom}H$), 7.84 (s, 1H, $C_{arom}H$), 7.93 (s, 1H, $C_{arom}H$), 7.98 (d, 2H, $C_{arom}H$), ∼12.6 (s, very broad, C_{arom}−OH and/or COOH), 16.97 (s, 1H, C_{enol}−OH).

^{13}C NMR ($CDCl_3$): δ (ppm) = 21.2 (CH_3), 128.3 (C_{arom}), 129.1 (C_{arom}), 130.2 (C_{arom}), 134.2 (C_{arom}), 136.0 (C_{arom}), 137.0 (C_{arom}), 160.2 (C_{arom}OH), 173.4 (C═O), 183.2 (C═O), 186.9 (COOH).

Anal. Calcd for $C_{17}H_{14}O_5$ (M_r = 298.30): C, 68.45; H, 4.73. Found: C, 68.21; H, 4.84.

ESI (*m*/*z*): 297, $[M - H]^-$.

$[Mn_2(HL1)_2(py)_4]$ (1). To a stirred, colorless solution of $Mn(OAc)_2{\cdot}4H_2O$ (62 mg, 0.25 mmol) in pyridine (10 mL) was added a yellow solution of H_3**L1** (100 mg, 0,25 mmol) in pyridine (10 mL). The solution turned orange, and the stirring was maintained for a few minutes. After this, Et_2O (10 mL) was added to the mixture and the reaction flask was stoppered and left undisturbed. After 2 days, large orange plate-shaped crystals had deposited, which were suitable for X-ray crystallography. The crystals were collected by filtration and dried in vacuo. The yield was quantitative.

IR (neat): ν (cm^{-1}) = 1598.2 w, 1587.0 w, 1548.9 s, 1505.6 vs, 1471.9 s, 1455.6 vs, 1435.7 vs, 1378.0 s, 1332.9 s, 1263.7 s, 1217.0 w, 1217.0 w, 1069.8 w, 1035.6 w, 811.9 w, 748.4 w, 698.1 vs, 668.1 s, 642.3 w, 614.0 s, 522.7 w, 476.2 w, 435.2 w, 415.9 w.

Anal. Calcd for **1** (*Mr* = 1223.12): C, 68.74; H, 4.61; N, 4.58. Found: C, 68.50; H, 4.57; N, 4.70.

$[Mn_3(HL1)_3]$ (2). Method 1. A mixture of H_3**L1** (50 mg, 0.13 mmol) and $Mn(OAc)_2{\cdot}4H_2O$ (30 mg, 0.13 mmol) was stirred in CH_2Cl_2 for 3 days. The fine suspension was filtered, and the yellow filtrate was layered with Et_2O/hexanes (1:1 in volume) for a few days. After this period, crystals of **2** were obtained, collected by filtration and dried in vacuo. The yield was 50%.

IR (neat): ν (cm^{-1}) = 1591.0 w, 1557.8 vs, 1505.3 vs, 1479.9 vs, 1455.8 s, 1417.5 vs, 1371.7 w, 1286.7 s, 1243.8 vs, 1179.9 w, 1062.9 w, 1026.1 w, 964.1 w, 953.5 w, 811.8 w, 785.9 vs, 714.4 s, 688.6 s, 646.1 s, 628.6 w, 560.1 vs, 542.8 s, 471.4 s, 378.5 w.

Anal. Calcd for **2** (M_r = 1360.07): C, 66.23; H, 4.00. Found: C, 66.25; H, 4.07.

Method 2. A solution of H_3**L1** (50 mg, 0.13 mmol) in pyridine (5 mL) was added to a solution of $Mn(OAc)_2{\cdot}4H_2O$ (30 mg, 0.13 mmol) in MeOH (5 mL), and the orange mixture was stirred for a few minutes, after which a yellow precipitate formed. The stirring was maintained for about 30 min, and then more MeOH (20 mL) was added to the mixture. The yellow powder was collected by filtration, dried in air, and dissolved in CH_2Cl_2 (15 mL). The resulting yellow solution was layered with a mixture of Et_2O/hexanes 1:1 in volume. After a few days, yellow needles of **2**, suitable for X-ray crystallography, were obtained, which were collected by filtration. The overall yield was ∼60%.

Anal. Calcd for **2**·0.2CH_2Cl_2 (M_r = 1377.06): C, 65.59; H, 3.98. Found: C, 65.61; H, 3.75.

Conversion of 2 into 1. Complex **2** (35 mg, 0.026 mmol) was dissolved in pyridine (6 mL) and stirred for a few minutes. The resulting orange solution was layered with Et_2O. After 1 week, block-shaped orange crystals of **1** were collected by filtration and dried in vacuo. The yield was 73%.

Anal. Calcd for **1**·py (M_r = 1302.23): C, 69.18; H, 4.72; N, 5.38. Found: C, 69.11; H, 4.98; N, 5.55.

Conversion of 1 into 2. Complex **1** (74 mg, 0. 061 mmol) was dissolved in CH_2Cl_2 (15 mL), and the solution was stirred for a few minutes. The resulting yellow solution was layered with a mixture of Et_2O/hexanes 1:1 in volume. After 10 days, yellow needles of **2** had deposited on the walls of the tube, which were collected by filtration and dried in vacuo. The yield was 86%.

Anal. Calcd for **2** (M_r = 1360.07): C, 66.23; H, 4.00. Found: C, 66.13; H, 4.07.

$[Mn_2(L2)_2(py)_4]$ (3). Method 1. To a stirred, dark brown solution of $NBu^n{}_4MnO_4$ (120 mg, 0.33 mmol) and $Mn(OAc)_2{\cdot}4H_2O$ (324 mg, 1.32 mmol) in DMF (20 mL) was added dropwise a solution of H_3**L1** (1000 mg, 2.50 mmol) in DMF (40 mL). The mixture was stirred for approximately 30 min, and then a fine brown precipitate was obtained upon addition of MeOH. The solid was collected by filtration and obtained in a mass of 813 mg after drying in air. Part of this crude (400 mg) was dissolved in pyridine (100 mL), and the solution was layered with Et_2O in various tubes. After 3 days, dark brown block-shaped crystals of pure **3** had formed on the walls of the tubes, which were suitable for X-ray crystallography. The crystals were collected by filtration before the crystallization of an orange byproduct started (this product was subsequently identified as **1**). The overall yield was calculated to be 9% on the basis of the total amount of Mn.

IR (neat): ν (cm^{-1}) = 1626.7 w, 1596.1 w, 1505.9 vs, 1480.4 s, 1436.3 vs, 1330.5 vs, 1280.4 s, 1210.6 s, 967.8 w, 832.8 s, 696.0 vs, 638.6 s, 623.9 s, 560.1 s, 545.9 s, 524.8 vs, 449.3 s, 363.9 vs, 327.9 s.

Anal. Calcd for **3**·1.2py (*Mr* = 1111.76): C, 64.82; H, 4.35; N, 6.55. Found: C, 64.45; H, 3.93; N, 6.99.

Method 2. To a stirred solution of $NBu^n{}_4MnO_4$ (25 mg, 0.07 mmol) and $Mn(OAc)_2{\cdot}4H_2O$ (67 mg, 0.27 mmol) in pyridine (15 mL) was added dropwise a yellow solution of H_3**L2** (100 mg, 0.34 mmol) in pyridine (15 mL). The mixture was stirred for a few

Table 1. Crystallographic Data for $[Mn_2(H\mathbf{L1})(py)_4]$ (**1**), $[Mn_3(H\mathbf{L1})_3]$ (**2**), and $[Mn_2(\mathbf{L2})_2(py)_4]$ (**3**)

param	**1**	**2**	**3**
formula	$C_{70}H_{56}Mn_2N_4O_{10}\cdot 5C_5H_5N$	$C_{75}H_{54}Mn_3O_{15}$[a]	$C_{54}H_{42}Mn_2N_4O_{10}$[a]
fw	1618.62	1360.01[a]	1016.80[a]
space group	*C*2/*c*	Pccn	$P\bar{1}$
a, Å	25.215(3)	21.998(3)	9.4178(10)
b, Å	15.166(2)	32.757(10)	10.7732(12)
c, Å	21.295(2)	20.784(3)	10.7732(12)
α, deg	90	90	94.584(10)
β, deg	91.455(9)	90	108.001(10)
γ, deg	90	90	100.489(10)
V, Å^3	8140.8(16)	14977(5)	1409.8(3)
Z	4	8	1
T, K	150	150	150
ρ_{calc}, g/cm^3	1.3207(2)	1.2063[a]	1.1976[a]
μ, mm^{-1}	0.398	0.558	0.503a
wR2[b]	0.1100	0.2216	0.1146
R^c ($I > 2\sigma(I)$)	0.0423 (5551 reflcns)	0.0956 (7734 reflcns)	0.0408 (4965 reflcns)
S	1.066	1.042	1.076

[a] No solvate molecules included. [b] $wR2 = [\sum[w(F_o^2 - F_c^2)^2]/\sum[w(F_o^2)^2]]^{1/2}$. [c] $R = \sum||F_o| - |F_c||/\sum|F_o|$.

minutes and then layered with Et_2O in various tubes. After 4 days, dark brown block-shaped crystals of pure **3** had formed on the walls of the tubes, which were collected by filtration and dried in vacuo. The yield was 70%.

Anal. Calcd for **3**·0.7py (*Mr* = 1072.21): C, 64.41; H, 4.28; N, 6.14. Found: C, 64.03; H, 4.43; N, 6.52.

X-ray Crystallography. Details of the crystal structure determinations of complexes **1** and **2** are given in refs 19 and 20, respectively. Selected crystallographic parameters have been included in Table 1.

For complex **3**, a dark brown, block-shaped crystal of approximate dimensions 0.09 × 0.15 × 0.30 mm, cut from a larger crystal, was mounted on a Lindemann-glass capillary and transferred into the cold nitrogen stream on a Nonius KappaCCD diffractometer on rotating anode. The unit-cell parameters were checked for the presence of higher lattice symmetry.[22] Crystal data and details on data collection are given in Table 1. Data were collected at 150 K using graphite-monochromated Mo Kα radiation ($\lambda = 0.710\ 73$ Å). In 6 h of X-ray exposure time, intensity data for 27 073 reflections were measured, 6417 of which were independent ($R_{int} = 0.0754$). The structure was solved by automated direct methods (SHELXS86)[23] and refined on F^2 using SHELXL-97.[24] Electron density in a disordered solvent area (a void of 356 Å^3, centered on the unit cell origin, probably filled with a mixture of pyridine and diethyl ether) was taken into account in the refinement via PLATON/SQUEEZE.[25] A total number of 101 electrons/unit cell was found in the solvent areas. Hydrogen atoms were included in the refinement on calculated positions riding on their carrier atoms. The methyl hydrogen atoms were refined as a rigid group, allowing for rotation around the C−C bond. All non-hydrogen atoms were refined with anisotropic thermal parameters. The hydrogen atoms were included in the refinement with a fixed isotropic thermal parameter related to the value of the equivalent isotropic displacement parameter of their carrier atoms. Final refinement included 317 parameters and a weighting scheme of $w^{-1} = \sigma^2(F_o^2) + (0.0616P)^2$, where $P = (\max(F_o^2,0) + 2F_c^2)/3$. Figures of merit are given in Table 1. No residual density was found outside −0.33 and 0.38 e Å^{-3}. Neutral atom scattering factors and anomalous dispersion corrections were taken from ref 26

Scheme 1

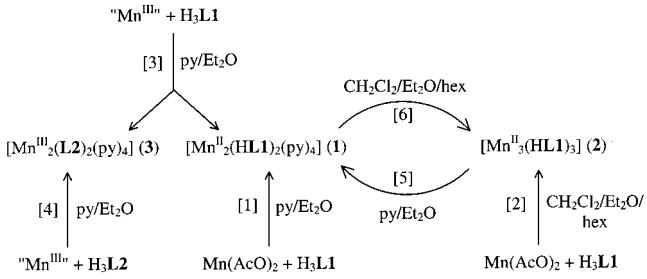

Physical Measurements. Infrared spectra were collected on a Perkin-Elmer Paragon 1000 spectrophotometer equipped with a Golden Gate Diamond ATR as a sample support. ^{1}H and ^{13}C NMR spectra were recorded on a 200 MHz JEOL JNM FX-200 instrument or a 300 MHz Bruker DPX 300 spectrometer. Chemical shifts are reported in the δ scale (parts per million) using the proton (^{1}H NMR) or the ^{13}C (^{13}C NMR) solvent signals, respectively, as references. Bulk magnetization measurements were carried out using a Quantum Design MPMS-5S SQUID magnetometer. Data were corrected for the magnetization of the sample holder. Diamagnetic contributions were calculated using Pascal's constants. Elemental analyses were performed in-house on a Perkin-Elmer Series II CHNS/O Analyzer 2400 or at the Microanalytical Laboratory of the University College, Dublin, Ireland.

Results and Discussion

Synthesis. The various coordination chemistry reactions presented in this section are summarized in Scheme 1 for clarity.

The O-pentadentate ligand $H_3\mathbf{L1}$ (vide supra)[11] was conceived to template the assembly of various transition metals into arrays as a way to prepare molecular species with interesting magnetic properties. Initial efforts in this direction involved reactions with Mn^{II}, since this ion in its high-spin configuration has the maximum possible number of unpaired electrons (d^5, $S = {}^5/_2$). The reaction between equimolar amounts of $H_3\mathbf{L1}$ and $Mn(OAc)_2$ in py/Et_2O afforded orange crystals of a dinuclear assembly with formula $[Mn_2(H\mathbf{L1})_2(py)_4]$ (**1**), as determined by X-ray crystallography (vide infra). In this reaction ([1] in Scheme 1), two of the three removable protons of H_3L have been ionized, most certainly to react with the acetate groups. The preference for the protons in α to the ketone groups is driven by the stability of the chelate rings that form during the process of complexation.

The preparation and identification of complex **1** raised the question of which molecular arrangement would be adopted by the $Mn^{II}/H_3\mathbf{L1}/AcO^-$ system in the absence of a coordinating solvent such as pyridine. Thus, the stoichiometric mixture of $H_3\mathbf{L1}$ and $Mn(OAc)_2$ was stirred for 3 days in CH_2Cl_2 and filtered. Crystals of a new complex were

(22) Spek, A. L. *J. Appl. Crystallogr.* **1988**, 578.
(23) Sheldrick, G. M. *SHELXL86 Program for crystal structure determination*; University of Göttingen: Göttingen, Germany, 1986.
(24) Sheldrick, G. M. *SHELXL-97 Program for crystal structure refinement*; University of Göttingen: Göttingen, Germany, 1997.
(25) Spek, A. L. *PLATON-A multipurpose crystallographic tool*; Utrecht University: Utrecht, The Netherlands, 2001. Internet: http://www.cryst.chem.uu.nl/platon.
(26) Wilson, A. J. C. *International Tables for Crystallography*; Kluwer Academic Publishers: Dordrecht, The Netherlands, 1992; Vol. C.

obtained from the filtrate, the microanalysis of which indicated the composition $[Mn(H\mathbf{L1})]_n$ (Scheme 1, reaction [2]). The X-ray single-crystal structure[19] of this new compound (vide infra) revealed a molecule with formula $[Mn_3(H\mathbf{L1})_3]$ (**2**) displaying a fascinating asymmetric triple-helical arrangement, which allows accommodation of three Mn^{II} ions within a distorted octahedral coordination sphere provided by three $(H\mathbf{L1})^{2-}$ donors, and no other ligands. With the formation of this molecule, showing a topology completely different from that of **1**, the versatility of the ligand $H_3\mathbf{L1}$ was revealed. Complex **2** was obtained in better yield by performing the reaction above in py/MeOH and recrystallizing the crude obtained this way.

The fact that Mn^{III} often forms complexes in its high-spin form (d^4, $S = 2$) and usually exhibits strong magnetic anisotropy[27,28] prompted us to investigate the reactivity of this ion with $H_3\mathbf{L1}$. For this, the comproportionation reaction (eq 1) between Mn^{II} and Mn^{VII} was employed to generate Mn^{III} in situ, by mixing the appropriate amounts of $Mn(OAc)_2$ and $NBu^n_4MnO_4$ in solution.

$$4Mn^{II} + Mn^{VII} \rightarrow 5Mn^{III} \quad (1)$$

The reaction of $H_3\mathbf{L1}$ with basic Mn^{III} in DMF leads to a brown precipitate upon addition of MeOH that was insoluble in most common organic solvents. Layers in Et_2O of this crude dissolved in pyridine produced black crystals of a compound that was different, as deduced by IR spectroscopy. Surprisingly, the X-ray structure of the crystalline compound (vide infra) revealed a Mn^{III} dinuclear complex, $[Mn_2(\mathbf{L2})_2(py)_4]$ (**3**), that did not contain the originally used ligand but instead a smaller ligand resulting from the degradation of the former. This new ligand, $(\mathbf{L2})^{3-}$ (see earlier structure), possessing a carboxylate residue in the place of a 3-oxo-3-phenylpropionyl group, can be viewed as the outcome of the oxidative cleavage of one of the 1,3-diketone units of $H_3\mathbf{L1}$. Such cleavages, catalyzed by transition metal ions, have been reported for cycloalkane-1,3-diones, which cannot act as chelates.[29] In the present case, however, this result was unexpected, given the abundance of complexes in the literature featuring the β-diketonate unit as a chelate of metals in high oxidation states. It is likely that, in this molecule, the presence of the phenol group near the diketone unit plays a crucial role in this cleavage, by allowing the coordination of Mn^{III} to only one of the carbonyl groups of that unit and assisting the dissociation. This is supported by the fact that a dinuclear complex of this ion with a ligand very similar to $H_3\mathbf{L1}$, lacking the phenolic hydroxide group, has been crystallographically characterized and no ligand degradation was observed.[15] If the mixtures yielding crystals of **3** were allowed to stand unperturbed for a longer period of time, the formation of a second phase, consisting of bunches of bright orange crystals, could be observed (see [3] in Scheme 1). The crystallization takes place in such a way that enough amounts of this second product could be separated from the whole system for its characterization. Elemental analysis, IR, and bulk magnetization measurements (vide infra) of this product allowed its to identification as complex **1**. This finding led to the assumption that the oxidizing equivalents necessary for the cleavage of $H_3\mathbf{L1}$, which resulted in the formation of **3**, came from one part of the Mn^{III} available in the system.

Table 2. Selected Interatomic Distances (Å) and Angles (deg) for $[Mn_2(H\mathbf{L1})_2(py)_4]$ (**1**)

Mn(1)···Mn(1)a	9.3018(13)	Mn(1)−N(7)	2.2415(17)
Mn(1)−O(2)	2.1522(15)	Mn(1)−N(8)	2.2631(16)
Mn(1)−O(3)	2.1651(14)	O(3)···O(4)	2.4753(19)
Mn(1)−O(5)a	2.1557(13)	O(4)−H(4)	0.81(2)
Mn(1)−O(6)a	2.1337(14)		
O(2)−Mn(1)−O(3)	79.96(5)	O(3)−Mn(1)−N(8)	169.43(6)
O(2)−Mn(1)−O(5)a	168.01(5)	O(5)a−Mn(1)−(6)a	82.95(5)
O(2)−Mn(1)−O(6)a	91.53(6)	N(7)−Mn(1)−O(5)a	90.46(6)
O(2)−Mn(1)−N(7)	95.01(6)	N(7)−Mn(1)−O(6)a	173.40(6)
O(2)−Mn(1)−N(8)	89.72(6)	N(7)−Mn(1)−N(8)	88.69(6)
O(3)−Mn(1)−O(5)a	89.39(5)	N(8)−Mn(1)−O(5)a	101.09(6)
O(3)−Mn(1)−O(6)a	90.32(5)	N(8)−Mn(1)−O(6)a	92.23(6)
O(3)−Mn(1)−N(7)	89.95(6)	O(3)−H(4)−O(4)	155(2)

Efforts for the direct preparation of **3** from its components were also undertaken. For this, a synthetic route to the ligand $H_3\mathbf{L2}$ was devised, since this compound is not described in the literature. This work was also motivated by the potential use that this new ligand may have in coordination chemistry. The new molecule was obtained following the Claisen condensation between 5-methyl-3-acetylsalicylic acid and ethyl benzoate. The former was obtained following a modification of a described procedure,[30] which consisted on the acylation of the OH group in 5-methylsalicylic acid using acidic anhydride, followed by intramolecular Friedel−Craft acylation of the resulting compound. The synthetic sequence leading to $H_3\mathbf{L2}$ involved the preparation of three new organic molecules, the full characterization of which is described in the Experimental Section. Complex **3** could be obtained as pure crystals in 70% yield from the reaction in pyridine of $H_3\mathbf{L2}$ with Mn^{III} ([4] in Scheme 1).

Description of the Structures. Crystallographic data for $[Mn_2(H\mathbf{L1})_2(py)_4]$ (**1**), $[Mn_3(H\mathbf{L1})_3]$ (**2**), and $[Mn_2(\mathbf{L2})_2(py)_4]$ (**3**) are collected in Table 1. Selected interatomic distances and angles for complexes **1**−**3** are listed in Tables 2−4. ORTEP and PLUTON representations of these complexes are shown in Figures 1−4.

$[Mn_2(HL1)_2(py)_4]$ (1). Complex **1** (Figure 1) contains two Mn^{II} ions chelated and bridged by two centrosymmetrically equivalent $(H\mathbf{L1})^{2-}$ ligands. The slightly distorted octahedral coordination geometry around each metal is completed by two terminal pyridine ligands, which lay in cis configuration. The Mn−N bond distances are 2.2415(17) and 2.2631(16) Å, respectively, and the Mn−O distances are in the range 2.1337(14)−2.1651(14) Å. The Mn···Mn separation is 9.3018(13) Å. The assignment of 2+ as the oxidation state of Mn is based on the coordination geometry[31] and charge

(27) Krzystek, J.; Telser, J.; Knapp, M. J.; Hendrickson, D. N.; Aromí, G.; Christou, G.; Angerhofer, A.; Brunel, L.-C. *Appl. Magn. Reson.* **2001**, *21*, 571.
(28) Barra, A. L.; Gatteschi, D.; Sessoli, R.; Abbati, G. L.; Cornia, A.; Fabretti, A. C.; Uytterhoeven, M. G. *Angew. Chem., Int. Ed. Engl.* **1997**, *36*, 2329.
(29) Cossy, J.; Belotti, D.; Bellosta, V.; Brocca, D. *Tetrahedron Lett.* **1994**, *35*, 6089.
(30) Zwaagstra, M. E.; Timmerman, H.; Abdoelgafoer, R. S.; Zhang, M. Q. *Eur. J. Med. Chem.* **1996**, *31*, 861.

Table 3. Selected Interatomic Distances (Å) and Angles (deg) for $[Mn_3(HL1)_3]$ (**2**)

Mn(1)···Mn(2)	3.0324(17)	Mn(2)−O(18)	2.116(4)
Mn(2)···Mn(3)	5.044(2)	Mn(2)−O(22)	2.116(4)
Mn(1)···Mn(3)	8.076(3)	Mn(2)−O(23)	2.118(4)
Mn(1)−O(11)	2.099(5)	Mn(3)−O(14)	2.218(4)
Mn(1)−O(12)	2.207(4)	Mn(3)−O(15)	2.092(4)
Mn(1)−O(16)	2.097(5)	Mn(3)−O(19)	2.261(4)
Mn(1)−O(17)	2.260(4)	Mn(3)−O(20)	2.093(4)
Mn(1)−O(21)	2.095(5)	Mn(3)−O(24)	2.172(4)
Mn(1)−O(22)	2.247(5)	Mn(3)−O(25)	2.143(4)
Mn(2)−O(12)	2.128(4)	O(13)···O(14)	2.409(6)
Mn(2)−O(13)	2.147(4)	O(18)···O(19)	2.382(6)
Mn(2)−O(17)	2.137(4)	O(23)···O(24)	2.385(6)
Mn(1)−Mn(2)−Mn(3)	179.20(3)	O(12)−Mn(1)−(21)	151.92(17)
O(11)−Mn(1)−O(12)	80.40(16)	O(12)−Mn(1)−(22)	76.38(16)
O(11)−Mn(1)−O(16)	99.65(18)	O(16)−Mn(1)−(17)	80.13(16)
O(11)−Mn(1)−O(17)	152.08(17)	O(16)−Mn(1)−(21)	98.45(18)
O(11)−Mn(1)−O(21)	92.96(18)	O(16)−Mn(1)−(22)	150.79(17)
O(11)−Mn(1)−O(22)	109.56(17)	O(17)−Mn(1)−(21)	114.78(17)
O(12)−Mn(1)−O(16)	109.53(17)	O(17)−Mn(1)−(22)	74.17(16)
O(12)−Mn(1)−O(17)	73.57(15)	O(21)−Mn(1)−(22)	80.35(17)
O(12)−Mn(2)−O(13)	80.95(16)	O(14)−Mn(3)−(15)	78.50(15)
O(12)−Mn(2)−O(17)	77.72(16)	O(14)−Mn(3)−(19)	78.80(14)
O(12)−Mn(2)−O(18)	114.47(16)	O(14)−Mn(3)−(20)	144.71(15)
O(12)−Mn(2)−O(22)	80.94(17)	O(14)−Mn(3)−(24)	82.40(15)
O(12)−Mn(2)−O(23)	153.83(16)	O(14)−Mn(3)−(25)	123.12(15)
O(13)−Mn(2)−O(17)	150.51(16)	O(15)−Mn(3)−(19)	116.91(15)
O(13)−Mn(2)−O(18)	89.11(15)	O(15)−Mn(3)−(20)	90.83(16)
O(13)−Mn(2)−O(22)	116.99(16)	O(15)−Mn(3)−(24)	147.75(16)
O(13)−Mn(2)−O(23)	90.87(16)	O(15)−Mn(3)−(25)	89.95(16)
O(17)−Mn(2)−O(18)	81.54(16)	O(19)−Mn(3)−(20)	76.37(15)
O(17)−Mn(2)−O(22)	79.46(17)	O(19)−Mn(3)−(24)	84.03(15)
O(18)−Mn(2)−O(22)	152.23(17)	O(19)−Mn(3)−(25)	149.55(15)
O(18)−Mn(2)−O(23)	90.02(16)	O(20)−Mn(3)−(24)	119.07(16)
O(17)−Mn(2)−O(23)	116.88(16)	O(20)−Mn(3)−(25)	89.99(16)
O(22)−Mn(2)−O(23)	80.80(17)	O(24)−Mn(3)−(25)	79.03(16)

Table 4. Selected Interatomic Distances (Å) and Angles (deg) for $[Mn_2(L2)_2(py)_4]$ (**3**)

Mn(1)···Mn(1)a	5.2614(7)	Mn(1)−N(61)	2.2945(17)
Mn(1)−O(11)	1.9318(12)	O(11)−C(13)	1.2983(19)
Mn(1)−O(21)a	1.8580(12)	O(12)−C(15)	1.285(2)
Mn(1)−O(12)	1.9334(12)	O(21)−C(22)	1.339(2)
Mn(1)−O(31)a	1.8980(13)	O(31)−C(33)	1.304(2)
Mn(1)−N(51)	2.3075(17)	O(32)−C(33)	1.222(2)
O(11)−Mn(1)−O(12)	89.65(5)	O(12)−Mn(1)−(61)	89.23(5)
O(11)−Mn(1)−O(21)a	176.83(5)	O(21)a−Mn(1)−(31)a	92.14(5)
O(11)−Mn(1)−O(31)a	90.95(5)	N(51)−Mn(1)−(21)a	92.94(5)
O(11)−Mn(1)−N(51)	87.69(5)	N(51)−Mn(1)−(31)a	91.36(6)
O(11)−Mn(1)−N(61)	86.23(5)	N(51)−Mn(1)−N(61)	173.41(5)
O(12)−Mn(1)−O(21)a	87.27(5)	N(61)−Mn(1)−(21)a	92.99(5)
O(12)−Mn(1)−O(31)a	179.22(5)	N(61)−Mn(1)−(31)a	91.31(6)
O(12)−Mn(1)−N(51)	88.17(5)		

considerations and is consistent with the magnetic properties of **1** (vide infra). Interestingly, the ligands in this complex are in anti−syn conformation with respect to their β-diketonate units (see Chart 1). It is worthwhile noting that the free ligand also exhibits this conformation in the solid state, as was revealed by the X-ray structure of the organic molecule.[20] It should be mentioned, however, that the Ni^{II} counterpart of complex **1** has also been characterized and it shows the $(HL1)^{2-}$ ligand in the syn−syn conformation, as induced, presumably, by the trans configuration favored at the Ni^{II} centers.[20] The polynucleating ligands in **1** are not completely planar, the angle between the idealized planes containing both β-diketonate units being 40.74(9)°. The phenolic hydrogen atom of H_3L1 is the only ionizable H moiety that remains on the ligand after complexation. This

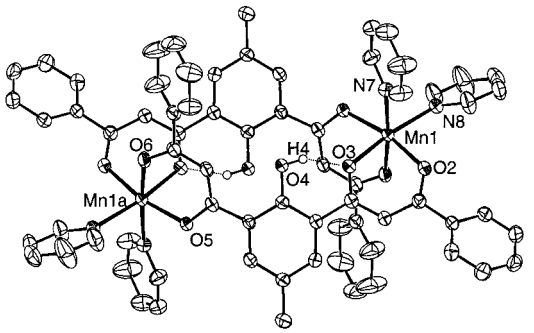

Figure 1. ORTEP representation of $[Mn_2(HL1)_2(py)_4]$ (**1**) at the 50% probability level. Only the hydrogen atoms involved in H-bonding are shown.

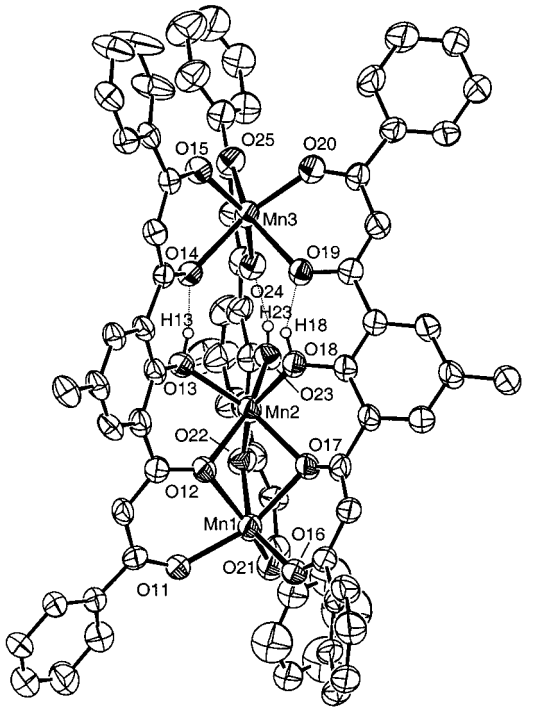

Figure 2. ORTEP representation of $[Mn_3(HL1)_3]$ (**2**) at the 40% probability level. Only the refined hydrogen atoms are shown.

has been confirmed by the crystal structure determination, since this proton has been located in the electron density map as a part of an intramolecular hydrogen bonding between O3 and O4, which displays a O3···O4 distance of 2.4753(19) Å. This separation is slightly shorter than the equivalent vector in the free ligand (2.497 Å) or other organic molecules containing a similar moiety[32,33] and falls within the range found in coordination complexes displaying the M−O−H···O−M unit.[34,35]

$[Mn_3(HL1)_3]$ (2). The molecule of **2** (Figure 2) features a trinuclear array of Mn^{II} ions chelated and bridged by three $(HL1)^{2-}$ ligands wrapped around the molecular axis in an

(31) Cotton, F. A.; Wilkinson, G. *Advanced Inorganic Chemistry*, 5th ed.; Wiley: New York, 1988.

(32) Jones, R. D. G. *Acta Crystallogr.* **1976**, *B32*, 301.

(33) Sugawara, T.; Mochida, T.; Miyazaki, A.; Akira, I.; Sato, N.; Sugawara, Y.; Deguchi, K.; Moritomo, Y.; Tokura, Y. *Solid State Commun.* **1992**, *83*, 665.

(34) Bertrand, J. A.; Black, T. D.; Eller, P. G.; Helm, F. T.; Mahmood, R. *Inorg. Chem.* **1976**, *12*, 2965.

(35) Nieuwpoort, G.; Verschoor, G. C.; Reedijk, J. *J. Chem. Soc., Dalton. Trans.* **1983**, 531.

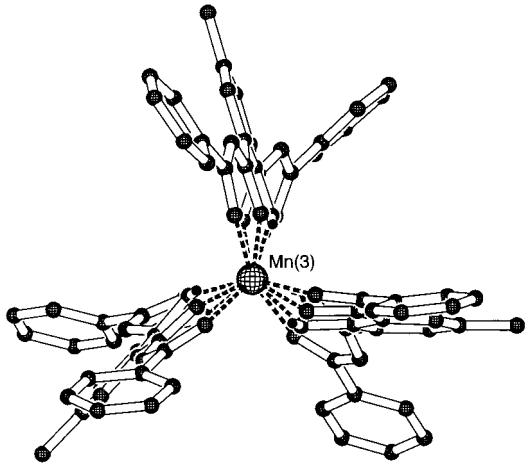

Figure 3. PLUTON representation of $[Mn_3(H\mathbf{L1})_3]$ (**2**) down the molecular axis.

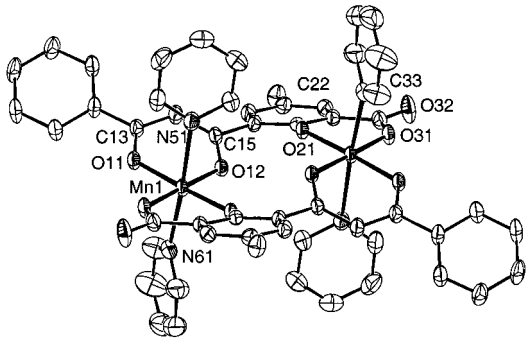

Figure 4. ORTEP representation of $[Mn_2(\mathbf{L2})_2(py)_4]$ (**3**) at the 50% probability level.

Chart 1

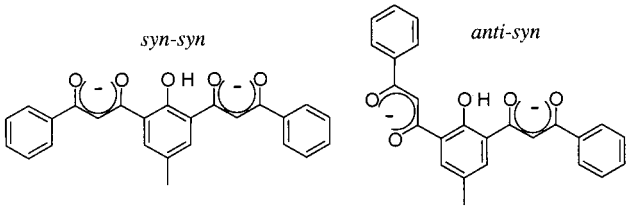

irregular helical manner. The three metal centers are quasi collinear (Figure 3; angle Mn1−Mn2−Mn3 = 179.20(3)°) and display three distinct Mn···Mn vectors with distances of 3.0324(17), 5.044(2), and 8.076(3) Å for Mn1···Mn2, Mn2···Mn3, and Mn1···Mn3, respectively. Each of the two peripheral metals of the complex is chelated by three β-diketonate units from the ligands. The central metal ion is bridged to Mn1 by the three inner oxygen donors of the corresponding diketonate groups, with the oxygen atoms from the phenol units completing the hexacoordination around this ion in form of six-membered chelate rings. In this arrangement, the manganese ions are accommodated in a coordination geometry that is intermediate between the octahedron and an ideal trigonal prism (vide infra), with Mn−O distances in the range 2.092(4)−2.261(4) Å range. The 2+ oxidation state of all the manganese ions in **2** is consistent with valence bond sum analysis, the elemental analysis of the compound, and its magnetic behavior (vide infra). Three intramolecular (O−H···O) hydrogen bonds have been crystallographically confirmed in this molecule[19] (one per ligand), analogous to what is found in complex **1**. These groups fill the cavity left between Mn2 and Mn3, and their presence is consistent with the electroneutrality of this complex. The distances of the O−H···O contacts, between O13, O18, O23 and O14, O19, O24, respectively, are 2.409(6), 2.382(6), and 2.385(6) Å. In contrast with complex **1**, the $(H\mathbf{L1})^{2-}$ ligands of **2** exhibit the syn−syn conformation (see Chart 1) of their β-diketonate groups and the angles between the idealized planes containing these two units within each ligand are 39.0(3), 34.3(3), and 21.9(3)°, respectively. The topological asymmetry of the three metals along the molecular axis is very rare among the family of metallohelicates.[10,36,37] In addition to complex **2**, it has also been observed recently in the trinuclear Ni^{II} complex of a N,O-based polytopic ligand (pd2am), $[Ni_3(pd2am)_3(H_2O)](NO_3)_3$.[38] The structure of **2** bears resemblance with that of a previously reported trinuclear complex with formula $[Mn_3(acac)_6]$ (acac = acetylacetonate anion).[39] In this compound however, the metals are distributed symmetrically along the molecular axis and the 1,3-diketonato groups from individual acac ligands are the only chelating units present.

Coordination Geometry of Mn^{II} in 2. The coordination geometry around the metal ions in complex **2** is distorted and lies between the octahedron and the trigonal prism. A quantitative measure of the separation of the coordination geometry at the metal centers from these ideal polyhedra can be obtained by calculating the so-called continuous symmetry measures (CSM's).[40,41] The CSM of a structure with respect to a given symmetry is defined as a normalized root-mean-square deviation, in a 0 to 100 scale, of the actual polyhedron from the closest ideal polyhedron with that symmetry. Therefore, it tends to zero as the observed structure approaches the perfect shape. The CSM values of the Mn coordination geometries in complex **2,** with respect to the octahedron and an ideal ML_6 trigonal prism where all nine L···L distances are the same, have been calculated. These are, in the CSM(octahedron)/CSM(prism) format, 5.28/5.02, 6.29/3.63, and 8.36/2.11 for Mn1, Mn2, and Mn3, respectively. For all three manganese centers, the geometry is closer to a prism than to an octahedron, although, for Mn1, the separation from both reference shapes is very similar. Thus, the geometry around this ion is very close to what is termed an isosymmetrical structure. The simplest path to convert a perfect octahedron into a perfect trigonal prism is the rotation of two opposite faces of the former with respect to each other around their C_3 axes by 60° (Bailar twist). To assess how removed is a distorted structure from a given distortion path between two reference polyhedra such as the Bailar twist, the CSM coordinates of this structure can be represented by a point on a symmetry map[42] along with the

(36) Albrecht, M. *Chem. Soc. Rev.* **1998**, *27*, 281.
(37) Albrecht, M. *Chem. Rew.* **2001**, *101*, 3457.
(38) Thompson, L. K.; Matthews, C. J.; Zhao, L.; Wilson, C.; Leech, M. A.; Howard, J. A. K. *J. Chem. Soc., Dalton Trans.* **2001**, 2258.
(39) Shibata, S.; Onuma, S.; Inoue, H. *Inorg. Chem.* **1985**, *24*, 1723.
(40) Zabrodsky, H.; Peleg, S.; Avnir, D. *J. Am. Chem. Soc.* **1992**, *114*, 7843.
(41) Pinsky, M.; Avnir, D. *Inorg. Chem.* **1998**, *37*, 5575.

curve for the path of interest. If the coordinates of the geometry around Mn1, Mn2, and Mn3, respectively, are represented on the "octahedron vs trigonal prism" symmetry map, it can be seen that these ions present distortions that fall very close to the ideal path described by the Bailar twist (see Figure S1 of the Supporting Information). The small deviations from that ideal path can be accounted for by the slight experimental dispersion observed for the Mn^{II}−O distances as well as the lack of perfect C_3 symmetry of the coordination geometries. For comparison, the CSM's of the previously reported complex $[Mn_3(acac)_6]$ (vide supra)[39] have been calculated. This compound displays two distinct coordination geometries. The ligand donors around the central Mn^{II} ion form an almost perfect octahedron (CSM(octahedron)/CSM(prism) = 2.20/14.76) while the external ions, which are crystallographically identical, display an almost ideal trigonal prism (16.16/0.80).

$[Mn_2(L2)_2(py)_4]$ (3). The structure of **3** (Figure 4) consists of a centrosymmetric dinuclear complex of two Mn^{III} ions held at a distance of 5.2614(7) Å by two $(\mathbf{L2})^{3-}$ ligands. Four adjacent oxygen donors from each ligand are chelating the metal ions at their equatorial positions (Mn−O distances 1.8580(12)−1.9334(12) Å). The axially elongated octahedral geometry around each Mn center is completed by two staggered pyridine ligands (Mn−N distances 2.3075(17) and 2.2945(17) Å). The marked Jahn−Teller distortion of the coordination geometry around Mn, as well as the magnetic properties of **3** (vide infra), support 3+ as the oxidation state of the metals. To ensure the electroneutrality of the complex, the dinucleating ligands need to be fully deprotonated. A bond distance of 1.222(2) Å suggests the C33−O32 group as the only carbonyl functionality present in the molecule, the remaining C−O bond distances (1.285(2)−1.339(2) Å) reflecting bond orders smaller than 2. Each molecule of **3** interacts with six neighboring complexes through three C−H···O hydrogen bonds involving O32 and O32′, respectively (see Figure S2 of the Supporting Information). By virtue of the crystallographic inversion center in this molecule, the idealized coordination equatorial planes of both Mn ions are mutually parallel, although they are shifted with respect to each other (their perpendicular separation being 1.471(4) Å). This reduces the possibility of having π-conjugation delocalized throughout the $(\mathbf{L2})^{3-}$ ligands. Another example has been reported in the literature of a complex with the same $[Mn^{III}_2O_8N_4]$ core[43] as **3**, which has the formula $[Mn_2(bhpp)_2(py)_4]$, where H_3bhpp is 1,3-bis(2-hydroxyphenyl)-1,3-propanedione. This ligand is also found triply deprotonated in the complex, binding the Mn^{III} centers at the equatorial positions. In this case, however, the functional groups providing the protons are one 1,3-diketone unit and two phenol groups. As in **3**, the axial pyridine ligands are present in a staggered conformation. The axial and equatorial bond distances of both complexes are comparable.

Magnetochemistry. The magnetic behavior of the new assemblies presented in this report has been examined by variable-temperature bulk magnetic susceptibility measurements. Magnetic susceptibility data were collected in the 2−300 K (**1** and **2**) or 2−275 K (**3**) temperature ranges under a constant magnetic field of 1 kG and were fit to the appropriate theoretical equations (vide infra). From these fits, the corresponding magnetic coupling parameters and g values characterizing these complexes were extracted.

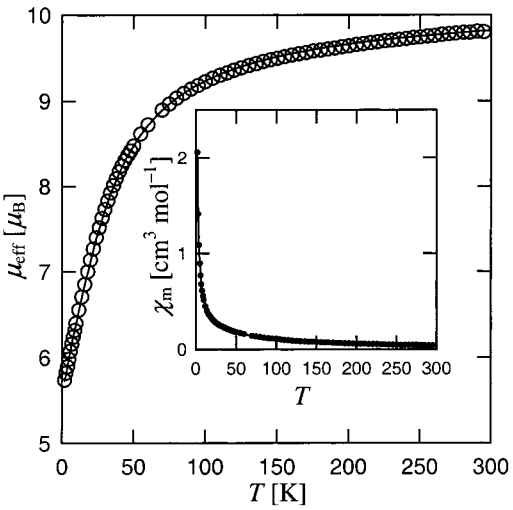

Figure 5. Plot of the effective moment, μ_{eff}, per molecule, versus temperature for $[Mn_3(H\mathbf{L1})_3]$ (**2**) in a 1 kG magnetic field. The solid line is the best fit to the experimental data (see text for details). Inset: Plot of the corresponding magnetic susceptibility versus T. The solid line represents the fit to the experimental data.

For complex **1**, the effective magnetic moment, μ_{eff}, remains practically constant over the entire range of temperatures (not shown). This indicates that the Mn^{II} ions of this dinuclear complex are not coupled magnetically. Indeed, the value of the magnetic moment (approximately 8.45 μ_B) is close to the expected spin-only value for two uncoupled Mn^{II} (d^5, $S = {}^5/_2$) ions with $g = 2$ (8.34 μ_B). The absence of magnetic coupling is not surprising in view of the crystal structure of this compound (Figure 1), which shows two Mn^{II} ions separated by a distance of 9.3018(2) Å and no apparent pathway for magnetic superexchange. To obtain an estimation of the g parameter, the experimental data where fit to the expression given in eq 2.

In this equation, S is the spin of a high-spin Mn^{II} ion ($S = {}^5/_2$), TIP is a temperature-independent paramagnetism parameter, and the rest of the terms have their usual meaning. From the linear regression of the experimental data the following best-fit parameters were obtained: $g = 2.01$; TIP $= 5.3 \times 10^{-4}$ cm^3 mol^{-1}.

$$\chi_m T = \frac{2Ng^2\mu_B{}^2}{3k} S(S+1) + (\mathrm{TIP})T \qquad (2)$$

A plot of μ_{eff}/molecule for complex **2** is shown in Figure 5. In this figure, the inset shows the experimental χ_m (magnetic susceptibility) vs T curve for this system. At room temperature, the magnetic moment has a value of 9.82 μ_B, very close to the expected spin-only number (10.25 μ_B) for three uncoupled high-spin Mn^{II} ions with $g = 2.00$ contained

(42) Alvarez, S.; Avnir, D.; Llunell, M.; Pinsky, M. *New J. Chem.*, submitted for publication.

(43) Casabo, J.; Colomer, J.; Escriche, L.; Teixidor, F.; Molins, E.; Miravitlles, C. *Inorg. Chim. Acta* **1990**, *178*, 221.

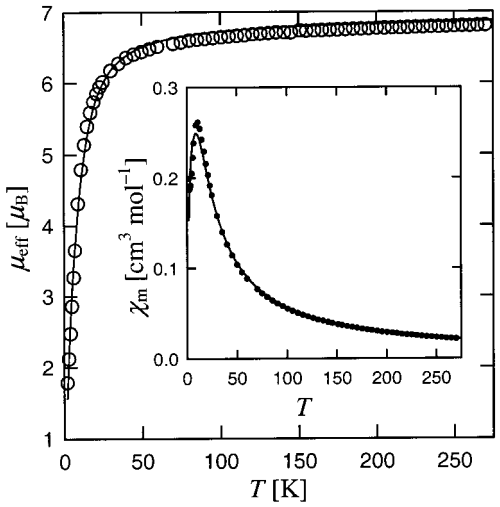

Figure 6. Plot of the effective moment, μ_{eff}, per molecule, versus temperature for $[Mn_2(\mathbf{L2})_2(py)_4]$ (**3**) in a 1 kG magnetic field. The solid line is the best fit to the experimental data (see text for details). Inset: Plot of the corresponding magnetic susceptibility versus *T*. The solid line represents the fit to the experimental data.

in the same molecule. The magnitude of μ_{eff} decreases monotonically with decreasing temperature to reach 5.74 μ_B at 2 K. This behavior is indicative of the existence of antiferromagnetic interactions within the molecule of **2**. A theoretical expression for the temperature dependence of χ_m in this system was obtained by considering a model that contemplates the presence of an exchange-coupled $Mn^{II}\cdots Mn^{II}$ pair next to a third, magnetically isolated Mn^{II} center. The details about the procedure used to fit the experimental data are given on a previous communication reporting the first preparation of this complex.[19] An excellent fit (solid lines in Figure 5) was obtained for the values $J = -2.75$ cm^{-1}, $g_{12} = 1.97$, and $g_3 = 1.92$, where J is the magnetic exchange coupling constant for the Mn_1Mn_2 pair and g_3 and g_{12} are the Landé factors of the Mn_3 ion and the Mn_1Mn_2 pair, respectively. The current fit has a slightly better quality than that previously communicated for this compound under a higher magnetic field (2 T), and the results are comparable. A detailed analysis of the χ_m vs T data by use of a full-matrix diagonalization method will be necessary to evaluate the importance of the three possible Mn2−O−H···O−Mn3 additional pathways of magnetic superexchange. However, the simplified model used above reproduces very well the experimental data. To the best of our knowledge, this would be the first molecular species containing two magnetically exchanged Mn^{II} ions next to a third, isolated Mn^{II} center. A detailed magnetic and EPR investigation of such system will be of relevance for the study of the active site of certain Mn-containing metalloenzymes such as the water oxidation complex of photosystem II, where a comparable [Mn_3 + Mn] arrangement is thought to exist.[44]

The experimental variation of μ_{eff} with respect to the temperature for complex **3** is shown in Figure 6. The value of μ_{eff}/μ_B ($\chi_m T$/cm^3 K mol^{-1}) remains practically constant at approximately 6.7 (5.6) over the whole temperature range until it starts to decrease abruptly at ∼60 K, to reach 1.8 (0.4) at 2 K. The value of μ_{eff} at the plateau is very close to the predicted number for a complex containing two magnetically isolated high-spin Mn^{III} (d^4, $S = 2$) ions with $g = 2$ (6.93 μ_B), whereas the drop at lower temperatures is consistent with the onset of a weak antiferromagnetic coupling within the molecule. This is also supported by the plot of magnetic susceptibility, χ_m vs T (Figure 6, inset), which shows a maximum at 11 K, indicative of the presence of such interaction. The experimental data were fit (solid lines in Figure 6) to a theoretical equation of χ_m vs T, derived by considering the energies that result from the following spin Hamiltonian:

$$\hat{H} = -2J\hat{S}_1 \tilde{S}_2 + \mu_B g \hat{S}_{12} \vec{B} - z2J' \langle S_{12z} \rangle \hat{S}_{12z} \qquad (3)$$

In the right-hand side of eq 3, the first term corresponds to the energy of the interaction between the electronic spins of the two Mn^{III} ions in **3**, the second is the Zeeman term for the states resulting from that coupling, and the third term accounts for the interaction between each complex and its neighboring molecules. In this Hamiltonian, S_i is the spin of Mn_i, with $S_1 = S_2 = 2$, J is the constant for the $Mn_1\cdots Mn_2$ spin−spin coupling, S_{12} is $S_1 + S_2$, z is the number of neighboring molecules interacting with each complex, $\langle S_{12z} \rangle$ is the mean value of the z component of S_{12}, and J' is the term of interaction between two nearest-neighbor molecules. The remaining terms have their usual meaning. The χ_m vs T expression for this system was obtained from the eigenvalues of the Hamiltonian as derived in the literature[45] for the case of a dinuclear cluster of two coupled transition metals displaying weak intermolecular interactions. This equation was fit to the experimental data by adjusting the parameters J, zJ', and g. The best fit was obtained for $J = -1.48$ cm^{-1}, $zJ' = 0.39$ cm^{-1}, and $g = 1.98$. A TIP value was included in the expression of the susceptibility and held constant at 400×10^{-6} cm^3 mol^{-1}. When the term for the intermolecular interaction was omitted from the Hamiltonian, the quality of the fit was considerably worse. The introduction of this term suggested the existence of a small ferromagnetic coupling between the magnetic states of neighboring molecules of **3**. Such exchange could be mediated by the intermolecular hydrogen-bonding interactions identified in the crystal structure (vide supra) and/or by dipolar interactions. The behavior of μ_{eff} at variable temperature, however, is, in light of this model, dominated by the antiferromagnetic interaction between both Mn^{III} centers, leading to a spin ground state of $S = 0$. Given the large separation between both Mn ions in **3** (5.2614(7) Å), the magnetic coupling between them cannot take place via direct overlap of their magnetic orbitals. Therefore, this coupling has to occur through a superexchange pathway, presumably involving the π orbitals of the bridging ligands and the metallic d orbitals with the appropriate symmetry. The related previously reported[43] complex $[Mn_2(bhpp)_2(py)_4]$ (vide supra), was found to exhibit significantly lower μ_{eff} vs T values. However, a comparison of those results with these reported here is not

(44) Zouni, A.; Witt, H. T.; Kern, J.; Fromme, P.; Krauss, N.; Saenger, W.; Orth, P. *Nature* **2001**, *409*, 739.

(45) Kahn, O. *Molecular Magnetism*; VCH: New York, 1993.

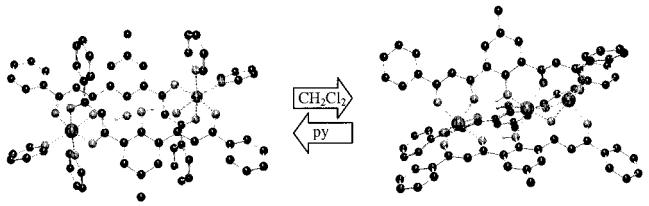

Figure 7. Scheme of the externally addressable switch formed by **1** and **2**.

possible since the authors did not indicate the units of their measurements.

The susceptibility data for **3** were also fit with a model that considered the presence of two uncoupled Mn^{III} ions, subject to axial ZFS, according to the single-ion Hamiltonian in eq 4.

In this Hamiltonian, S is the spin of a high-spin Mn^{III} ion ($S = 2$), D is the single-ion axial ZFS parameter, and the rest of the terms have the usual meanings. A less satisfactory fit was obtained using this model (see Figure S3 of the Supporting Information), with fitting parameters of $g = 2.04$ and $D = 4.30$ cm^{-1} and a constant TIP value of 400×10^{-6} cm^3 mol^{-1} for the dinuclear complex. Such a high, positive value of D is unusual for Mn^{III}.[27] For this reason, the first model, which also gives a better fit, is preferred. A detailed high-field EPR study is planned to discern between these two possibilities.

$$\hat{H} = \mu_B g \hat{S} \vec{B} + D\hat{S}_z^2 \qquad (4)$$

Solvent-Controlled Interconversion between 1 and 2. The isolation and characterization of complexes **1** and **2** remarkably demonstrate the versatility of the $Mn^{II}/(H\mathbf{L1})^{2-}$ system, whose molecular information can be expressed in the form of either of two discrete species with different topologies and magnetic properties, depending on the nature of the solvent used. In light of these results, it was thought that the kinetic lability of Mn^{II} would allow one to reversibly interconvert these two complexes by using external stimuli. Indeed, if the trinuclear complex **2** is dissolved in pyridine and the resulting orange solution is layered with Et_2O, crystals of pure **1** are obtained in high yield after a few days. This shows that complex **1** is more stable than **2** in pyridine and that the multiple dissociation and rearrangement steps necessary for this conversion (reaction [5] of Scheme 1) are kinetically accessible under the reaction conditions. The conversion in the opposite direction was likewise explored. Thus, if the dinuclear complex **1** is dissolved in CH_2Cl_2, a yellow solution is obtained after a few minutes. Layering of this solution with Et_2O/hexane results in the formation of crystals of **2** in high yield. This proves that if pyridine is not present in a large excess, complex **2** is the most stable species and that its formation from **1** (reaction [6] of Scheme 1) is also feasible kinetically. The above observations demonstrate that complexes **1** and **2** constitute a binary molecular switch that can be externally addressed by controlling the nature of the solvent medium (Figure 7). A similar system has been reported which affords either a tetranuclear or a hexanuclear Cu^{II} assembly, depending on the amount of acetonitrile present.[46] In the work reported here, in addition of structurally distinct architectures, the two states of the switch are two magnetic entities displaying different properties. In one case the assembly possesses two uncoupled Mn^{II} ions, and in the other it is formed by two exchange coupled Mn^{II} centers next to a third, magnetically independent Mn^{II} ion. Thus, this system represents an important contribution to the growing field known as adaptive chemistry,[47] by which complex chemical systems are described, capable of delivering different responses to a variety of environmental stimuli. Other important examples exist in the area of coordination supramolecular chemistry, where the nature of the species resulting from the self-assembly process depends on external factors, such as the type of anion present,[48] the nature of the cation,[49] or the incidence of light.[50]

Conclusions

In this work, the coordination properties of the new polynucleating ligand $H_3\mathbf{L1}$ with Mn^{II} and Mn^{III} have been presented. The versatility of the ligand $H_3\mathbf{L1}$ as a host for the multicomponent self-assembly of complex structures has been demonstrated by the isolation of two Mn^{II}-containing assemblies, $[Mn_2(H\mathbf{L1})_2(py)_4]$ (**1**) and $[Mn_3(H\mathbf{L1})_3]$ (**2**). Complex **2** represents an entirely new topology within the context of coordination helicates, chiefly due to its asymmetric disposition of the metals along the molecular axis. The $Mn^{II}/H_3\mathbf{L1}$ system presented here does not only afford structural diversity in terms of the architectures arising from the self-assembly of its components but also it is expressed in form of two species presenting different magnetic properties. Complex **1** possesses two magnetically independent Mn^{II} ions, and **2** features a pair of antiferromagnetically coupled Mn^{II} centers along with a third, magnetically isolated Mn^{II} ion. In addition, each of the two assemblies identified can be addressed by environmental stimuli (in this case the solvent medium) to be reversibly interconverted. It has been shown in addition that the system $Mn^{III}/H_3\mathbf{L1}$ in pyridine is unstable toward ligand degradation. This process leads to the oxidative cleavage of one of the β-diketone units of $H_3\mathbf{L1}$ to form the smaller donor $H_3\mathbf{L2}$, which features only one β-diketone group bound to one molecule of salicylic acid. This is revealed by the crystal structure of the new dinuclear complex $[Mn_2(\mathbf{L2})_2(py)_4]$ (**3**). According to the most satisfactory model, the coupling between the Mn^{III} centers in **3** is antiferromagnetic. The identification of the second inorganic product from this reaction as **1** points toward Mn^{III} as

(46) Baxter, P. N. W.; Khoury, R. G.; Lehn, J.-M.; Baum, G.; Fenske, D. *Chem.—Eur. J.* **2000**, *6*, 4140.
(47) Lehn, J.-M. In *Supramolecular Science: Where It Is and Where It Is Going*; Ungaro, R., Dalcanale, E., Eds.; Kluwer: Amsterdam, 1999.
(48) Hasenknopf, B.; Lehn, J.-M.; Boumediene, N.; Dupont-Gervais, A.; VanDorsselaer, A.; Kneisel, B.; Fenske, D. *J. Am. Chem. Soc.* **1997**, *119*, 10956.
(49) Scherer, M.; Caulder, D. L.; Johnson, D. W.; Raymond, K. N. *Angew. Chem., Int. Ed. Engl.* **1999**, *38*, 1588.
(50) Ratera, I.; Ruiz-Molina, D.; Vidal-Gancedo, J.; Wurst, K.; Daro, N.; Letard, J. F.; Rovira, C.; Veciana, J. *Angew. Chem., Int. Ed.* **2001**, *40*, 919.

the oxidizing agent during the cleavage of H_3**L1**. Complex **3** has been prepared in pure form and high yields, directly from its components. For this, the synthesis of the new ligand H_3**L2** has been designed and executed as described in this report. The potential of this donor as a template to direct the assembly of transition metal triads is currently under investigation.

Acknowledgment. Financial support by the European Union, under Contracts HPMF-CT-1999-00113 (Marie Curie Fellowship) to G.A. and TMR ERB-FMNRX-CT98-0199 to O.R., the NRSC (P.G.), the WFMO (J.R), and the CW-NWO (A.L.S.) is thankfully acknowledged. The authors are thankful to Dr. Pere Alemany i Cahner for continuous symmetry measure calculations and for helpful discussions in interpreting the results from these calculations.

Supporting Information Available: An X-ray crystallographic file for **3** in CIF format, the CSM map for the Bailar twist distortion between an octahedron and a trigonal prism containing the coordinates for the Mn^{II} in complex **2** (Figure S1), a figure showing the intermolecular interactions in complex **3** (Figure S2), and the magnetic data for complex **3** fit with a single-ion ZFS model (Figure S3). This material is available free of charge via the Internet at http://pubs/acs/org.

IC0200491